CHEMISTRY
A EUROPEAN JOURNAL

DOI: 10.1002/chem.200800750

Is an M−N σ-Bond Insertion Route a Viable Alternative to the M=N [2+2] Cycloaddition Route in Intramolecular Aminoallene Hydroamination/Cyclisation Catalysed by Neutral Zirconium Bis(amido) Complexes? A Computational Mechanistic Study

Sven Tobisch*[a]

Abstract: This study examines alternative reaction channels for intramolecular hydroamination/cyclisation (IHC) of primary 4,5-hexadien-1-ylamine aminoallene (**1**) by a neutral [Cp_2ZrMe_2] zirconocene precatalyst (**2**) by using the density functional theory (DFT) method. The first channel proceeds through a [$Cp_2Zr(NHR)_2$] complex as the reactive species and relevant steps including the insertion of an allenic C=C linkage into the Zr−NHR σ-bond and ensuing protonolysis. This is contrasted to the [2+2] cycloaddition mechanism involving a [Cp_2Zr=NR] transient species. The salient features of the rival mechanisms are disclosed. The cycloaddition route entails the first transformation of the dormant [$Cp_2Zr(NHR)_2$] complex **3B** into the transient [Cp_2Zr=NR] intermediate **3A′**, which is turnover limiting. This route features a highly facile ring closure together with a substantially slower protonolysis ($k_{cycloadd} \gg k_{protonolysis}$) and can display inhibition by high substrate concentration. In contrast, protonolysis is the more facile step for the channel proceeding through the [$Cp_2Zr(NHR)_2$] complex as the catalytically active species. Here, C=C insertion into the Zr−C σ-bond of **3B**, which represents the catalyst resting state, is turnover limiting and substrate concentration is unlikely to influence the rate. The regulation of the selectivity is elucidated for the two channels. DFT predicts that five-ring allylamine and six-ring imine are generated upon traversing the cycloaddition route, thereby comparing favourably with experiment, whereas the cycloimine should be formed solely along the σ-bond insertion route. The mechanistic analysis is indicative of an operating [2+2] cycloaddition mechanism. The Zr−NHR σ-bond insertion route, although appearing not to be employed for the reactants studied herein, is clearly suggested as being viable for hydroamination by charge neutral organozirconium compounds.

Keywords: allenes · density functional calculations · hydroamination · reaction mechanisms · zirconium

Introduction

Catalytic hydroamination, that is, the direct addition of amine R_2N−H bonds across unsaturated carbon-carbon functionalities, is a valuable, desirable and atom-economical means of synthesising organonitrogen compounds.[1] The intramolecular hydroamination/cyclisation (IHC) constitutes a particularly powerful route for the generation of functionalised azacycles. Group 4 metal complexes have been demonstrated to efficiently effect the IHC of various amine-tethered unsaturated carbon-carbon linkages.[2,3] Titanium- and zirconium-based catalysts benefit from their availability and easy preparation, in contrast to organolanthanide compounds,[4] which have also been widely explored as catalysts for this process.[5]

Although there are numerous accounts that describe the application of titanium and zirconium complexes in cyclohydroamination catalysis, the identity of the catalytically active species, namely, whether it possesses a metal–nitrogen single or double bond, is in most cases not unambiguously identified and thus largely speculated upon. Neutral Group 4 metal compounds[2,6,7] are commonly believed to engage a reactive metal-imido species, involving [2+2] cycloaddition of the unsaturated CC linkage across the M=N bond and subsequent protonolytic cleavage of the metallacyclobutane/butene intermediate. This mechanistic pathway was original-

[a] Dr. S. Tobisch
University of St Andrews, School of Chemistry
Purdie Building, North Haugh
St Andrews, Fife KY16 9ST (UK)
Fax: (+44) 1707-383-652
E-mail: st40@st-andrews.ac.uk

Supporting information for this article is available on the WWW under http://dx.doi.org/10.1002/chem.200800750.

ly proposed by Bergman and co-workers for intermolecular alkyne and allene hydroamination with primary amines mediated by zirconocene compounds[8] and was later extended to cyclohydroamination.[6] Various experimental studies,[9] of which the detailed kinetic investigation of Doye[9a] is most notable, and also computational[10] examination have substantiated this mechanism. Cationic Group 4 metal precatalysts, on the other hand, are likely to follow a different route employing a metal-amido active species,[3] a mechanism that was first proposed by Marks for organolanthanides.[5b,11] A computational survey of aminoallene IHC by a cationic zirconocene-amido species revealed a smooth energy profile, which is consistent with observed activity and selectivity.[12] Recently, Mark's group provided the first compelling evidence for an M–N σ-bond insertion route operating for aminoalkene IHC mediated by charge-neutral Zr complexes.[13,14]

The ambiguity as to whether the catalytically active species in hydroamination mediated by neutral Group 4 metal precatalysts actually bears a metal–nitrogen single or double bond prompted a computational exploration of alternative reaction channels by considering aminoallene IHC as an experimentally well studied reaction. Neutral titanium and zirconium compounds have been reported as being capable of promoting the cyclohydroamination of aminoallenes to furnish functionalised five- and six-membered azacycles.[15,16] As an example, zirconocene precatalyst **2** has been shown to promote the conversion of 4,5-hexadien-1-ylamine (**1**), albeit not regioselectively, into the six-membered imine as the predominant cycloamine (Scheme 1).[15b]

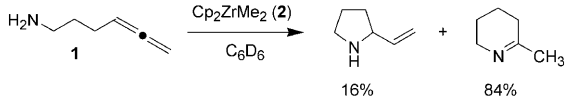

Scheme 1.

The computational survey of the plausible reaction channels shown in Scheme 2 employed the DFT method as an established and predictive means to aid in mechanistic understanding. The present study examines the channel proceeding through the $[Cp_2Zr(NHR)_2]$ complex (channel B in Scheme 2) and characterises all relevant elementary steps, both structurally and energetically. In a companion contribution we have recently communicated the salient features of the cycle that engages the $[Cp_2Zr{=}NR]$ intermediate (channel A in Scheme 2).[17] The free-energy profiles of the two channels are critically analysed and compared with experimental observation. Herein we show that Zr–N σ-bond insertion, although not being employed for the studied reaction partners, is still viable for aminoallene IHC mediated by neutral zirconium complexes. The present study, therefore, contributes towards a more detailed mechanistic understanding and enhances insight into the catalytic structure–reactivity relationship in Group 4 metal-mediated cyclohydroamination.

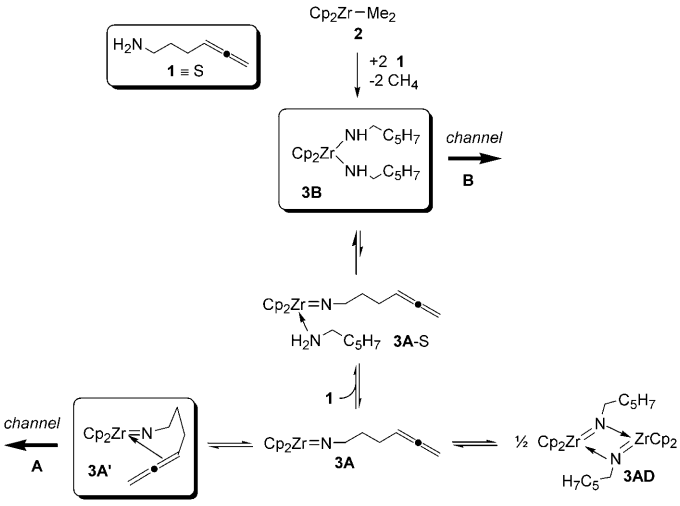

Scheme 2. Plausible alternative reaction channels for intramolecular hydroamination/cyclisation mediated by a charge-neutral zirconocene precatalyst. 4,5-Hexadien-1-yl-amine **1** and $[Cp_2ZrMe_2]$ compound **2** were chosen as archetypical terminal aminoallene substrate and precatalyst, respectively.

Results and Discussion

The mechanistic examination starts with the assessment of plausible routes for transformation of precatalyst **2** into $[Cp_2Zr{=}NR]$ and $[Cp_2Zr(NHR)_2]$ compounds. This is followed by the exploration of reaction channel B shown in Scheme 4, whereas the main mechanistic features of channel A, as unveiled in a recent computational study,[17] are summarised thereafter. The discussion will concentrate primarily on the most favourable of the several conceivable pathways for each step, whereas alternative, but less probable, pathways are referred to only briefly. The full account of the examined pathways is provided in the Supporting Information (Tables S1 and S2; Figures S1–S8). Finally, the reaction profiles of the two channels are compared with experimental evidence.

Conversion of precatalyst 2 into $[Cp_2Zr{=}NR]$ and $[Cp_2Zr(NHR)_2]$ compounds: Plausible routes have already been examined previously[17] and major conclusions are recalled here briefly. As revealed from the free energy profile shown in Scheme 3[18] the dominant route involves protonolytic cleavage of the two Zr–Me bonds in **2** by **1** to furnish first the $[Cp_2Zr{=}NR]$ intermediate (**2**+**1**→**I1**(+CH_4)→**3A**⇄**3A′**(+2CH_4)), which is consistent with experimental observation.[19a] The substrate-free forms of $[Cp_2Zr{=}NR]$ with a monohapto (**3A**) or chelating (**3A′**) imidoallene unit are rapidly interconvertible[20] and complex additional **1** readily to yield the adduct **3A**-S in an exergonic and barrierless process.[20] Subsequent proton shift between amido and amino units converts **3A**-S into **3B**.

The **I1**→**3A**⇄**3A′**+CH_4 α-elimination of methane is the step with the highest barrier along the most accessible route for transformation of **2** into imido- and bis(amido)-zircono-

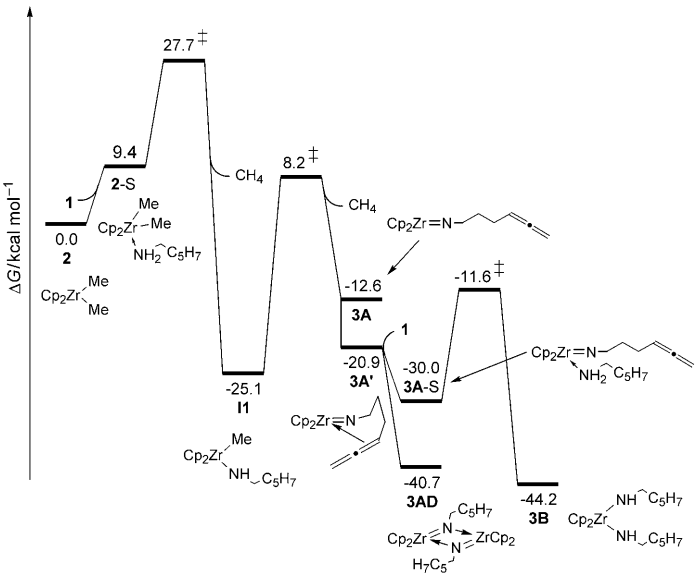

Scheme 3. Condensed free-energy profile for conversion of precatalyst **2** into $[Cp_2Zr{=}NR]$ and $[Cp_2Zr(NHR)_2]$ compounds.[18]

cenes. The computed free energy of activation of 33.3 kcal mol^{-1} (Scheme 3) agrees well with the measured rate constant for a similar zirconocene transformation.[21]

The bis(amido)-Zr complex **3B** is found to be the most stable of all compounds participating in plausible precatalyst transformation steps. Its formation is driven by a substantial thermodynamic force of 44.2 kcal mol^{-1}, hence **2** is transformed initially into **3B** almost quantitatively. It has been demonstrated experimentally that stable bis(amido)-zirconocenes undergo a reversible transformation into $[Cp_2Zr{=}NR]$ intermediates through the α-abstraction of amine.[19] This equilibrium is far to the left, but its kinetics have not been communicated. Indeed, the imido-zirconocene substrate adduct **3A**-S is found to be 14.2 kcal mol^{-1} higher in free energy than **3B** and the substrate free **3A′** is 23.3 kcal mol^{-1} above, thereby indicating that **3A′** is a transient species.[22] However, a substantial barrier of 32.6 kcal mol^{-1} ($\Delta G^{\ddagger}$ for **3B**⇄**3A**-S⇄**3A′**+**1**, Scheme 3) is associated with the transformation of the abundant $[Cp_2Zr(NHR)_2]$ complex into $[Cp_2Zr{=}NR]$ intermediates.

Reaction channel proceeding through the $[Cp_2Zr(NHR)_2]$ complex: Scheme 4 shows a plausible catalytic cycle proceeding through the $[Cp_2Zr(NHR)_2]$ compound **3B**. Insertion of an allenic C=C linkage into a Zr–NHR σ-bond gives rise to five- and six-membered azacyclic intermediates **4B** and **5B** bearing a functionalised tether, following 5-*exo* and 6-*endo* paths, respectively. The azacycle of the 6-*endo* cyclisation intermediate can interact with the Zr centre through its *N*-donor functionality (**5B**) or by an allylic interaction (**5B′**). These forms are likely to be readily interconvertible, that is **5B**⇄**5B′**. The successive transfer of a proton from the second amidoallene unit in **4B** and **5B**⇄**5B′** yields first cycloamine-imido-Zr compounds **7B** and **10B**, **11B**. Alternatively, protonolysis by **1** generates cycloamine-bis(amido)-Zr compounds **6B** and **8B**, **9B** (Scheme 7).[23] Intramolecular proton transfer onto the C^6 centre in **4B** furnishes first **7B**, from which **1** liberates 2-vinyl-pyrroline **P10**, thereby completing the catalytic cycle by regenerating **3B** via **3A**-S. The alternative protonolysis of the Zr–C^6 bond in **4B** by **1** affords **6B** from which **P10** is readily released to rebuild **3B**. The regioisomeric paths for intramolecular protonation at C^5 and C^7 centres in **5B**⇄**5B′** lead initially to 2-methylenepiperidine **P12** and 6-methyl-1,2,3,4-tetrahydropyridine **P11** by passing through **11B** and **10B**, respectively. Other plausible

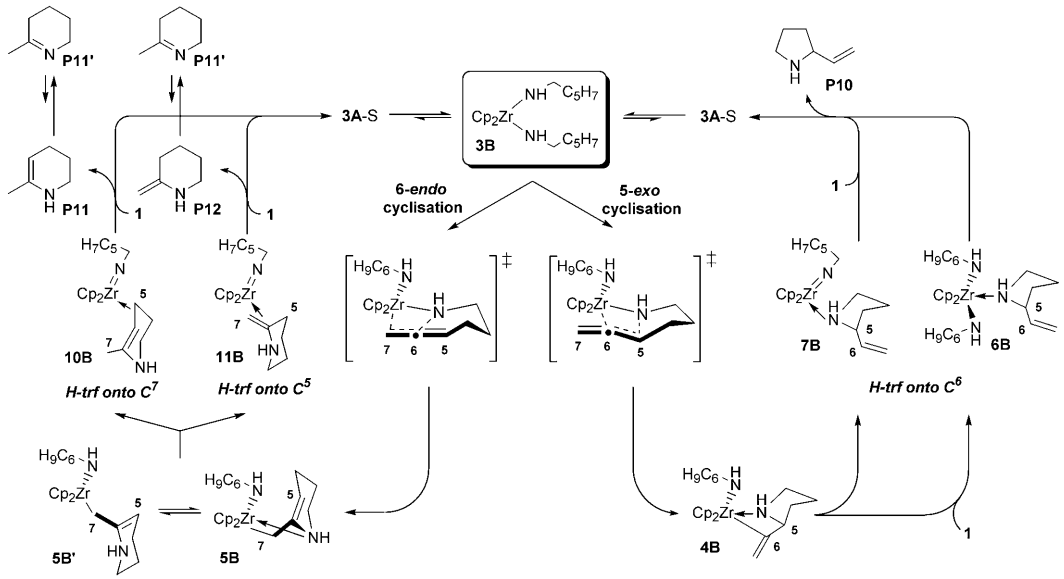

Scheme 4. Reaction channel proceeding through the bis(amido)-zirconocene complex **3B** in aminoallene IHC to afford functionalised five- and six-membered azacycles, based on experimental[5b,11,13] and computational[12] mechanistic studies.[23]

pathways via cycloamine-bis(amido)-Zr intermediates (**8B**, **9B**, Scheme 7) have been omitted for the sake of clarity. Cycloamines **P11** and **P12** are subsequently converted into the thermodynamically favourable 2-methyl-3,4,5,6-tetrahydropyridine **P11′** through a 1,3-hydrogen shift.

Intramolecular cyclisation: After precatalyst **2** is quantitatively transformed into **3B**, C–N bond formation through intramolecular addition of an allenic C=C linkage across the Zr–NHR σ-bond is the first step of the catalytic cycle. The bis(amido)-Zr complex **3B** prefers to have two monohapto amidoallene units. Other forms in which I) one or both amidoallene groups are linked to Zr in a chelating fashion through nitrogen and an allenic double bond, or II) a substrate adduct could not be located. This is understandable, because the suitable orbitals are involved in bonding to the two strong π-donating amido groups,[24] a state which is much preferred to an allenic double bond or amine molecule.

Two trajectories are conceivable for cyclisation (Scheme 5);[25] firstly, the frontal approach of the C=C double bond along the ring-centroid-Zr-ring-centroid bisector, and secondly, the lateral approach along the perpendicular to the ring-centroid-Zr-ring-centroid plane. Ring closure along the exocyclic pathway is found to proceed exclusively by the lateral approach, whereas the two trajectories towards the six-membered azacycle are almost degenerate energetically (Table S1 and Figure S1 in the Supporting Information). Unfavourable interactions between the azacycle's vinyl tether and the second amido ligand together with the trans disposition of two nitrogen donor centres are seen to disfavour transition state (TS) TS[**3B**-**4B**] along the frontal approach (Figure S1 in the Supporting Information). The following discussion will thus concentrate on the lateral approach for the regioisomeric 5-*exo* and 6-*endo* pathways.

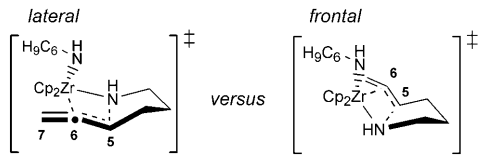

Scheme 5.

These are characterised structurally in Figure 1, whereas the energy profiles are collated in Table 1.

Cyclisation proceeds through a chair-like transition-state structures occurring at a distance of 2.14 Å for the emerging

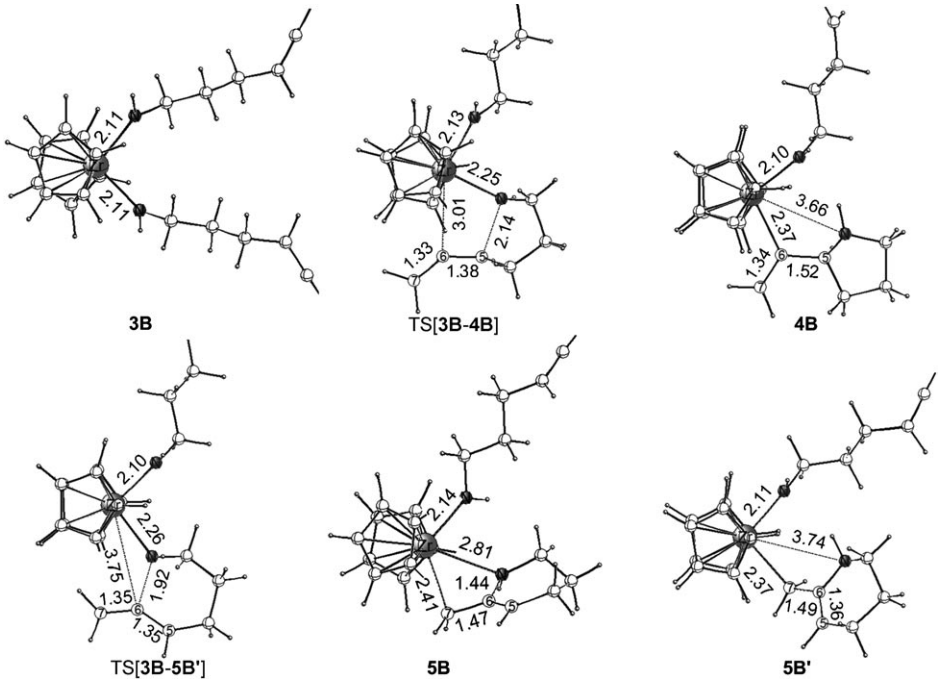

Figure 1. Selected structural parameters [Å] of the optimised structures of key stationary points for 5-*exo* (top) and 6-*endo* (bottom) cyclisation of **3B**. The cut-off for drawing Zr–C bonds was arbitrarily set to 2.8 Å. Note that the amidoallene units are displayed in a truncated fashion for several of the species.

Table 1. Enthalpies and free energies of activation and reaction for cyclisation of **3B** through regioisomeric 5-*exo* and 6-*endo* pathways.[a–c]

Cyclisation pathway	Precursor	TS	Product[d]
5-*exo*	0.0/*0.0* (**3B**)	35.4/*36.6*	4.3/*5.8* (**4B**)
6-*endo*	0.0/*0.0* (**3B**)	27.4/*29.2*	−2.4/*−0.6* (**5B**)
			−13.6/*−11.8* (**5B′**)

[a] See Scheme 4. [b] Enthalpies and free energies of activation ($\Delta H^{\neq}$/$\Delta G^{\neq}$) and reaction (ΔH/ΔG) are given in kilocalories per mole; the numbers in italic type are the Gibbs free energies. [c] The most accessible paths are referred to. See also Table S1. [d] See the text (or Figure 1 and S1) for a description of the azacyclic intermediates.

C–N bond in TS[**3B**-**4B**] and somewhat later at 1.92 Å in TS[**3B**-**5B**], which appears more product-like. Ring closure in **3B** does not benefit from the stabilisation of the TS structure by an azacyle's vinyl tether (5-*exo*) or allylic functionality (6-*endo*) that is closely attached to Zr, as discovered previously for a cationic $[Cp_2Zr–NHR]^+$ complex.[12] Similarly, this is prevented on electronic grounds by the presence of a strong π-donating amido spectator ligand. As a result, intramolecular cyclisation in **3B** is kinetically challenging and has a barrier of 29.2 kcal mol^{-1} ($\Delta G^{\neq}$) for the favoured 6-*endo* pathway.

Following this pathway further leads initially to **5B**, in which the azacycle interacts with Zr through its N-donor

and allylic C^7 centres. Transient species **5B** transforms readily into the more stable **5B′**, which has the azacycle coordinated exclusively by its allylic C^7 centre to Zr (Figure 1). Several modes are conceivable for an allylic azacycle ligation. It comes as no surprise that an η^1-C^7-allylic interaction is favoured versus an η^3-allylic ligation by 9.2 kcal mol^{-1} in the presence of the second amido ligand. All these forms are supposedly in a dynamic equilibrium.[26] The **3B**→**5B′** cyclisation is driven by a thermodynamic force of −11.8 kcal mol^{-1} and is therefore likely to proceed in an irreversible fashion. On the other hand, exocyclic **3B**→**4B** ring closure is endergonic ($\Delta G = 5.8$ kcal mol^{-1}) and is connected with a free-energy of activation that amounts to 36.6 kcal mol^{-1} (Table 1). The most stable form of **4B** sees the azacycle bound to Zr exclusively by its vinylic C^6 centre, whereas another form, which has the azacycle ligated by its N-donor centre and a somewhat more distant C^5 centre, is slightly higher in energy ($\Delta G = 1.6$ kcal mol^{-1}, Table S1 in the Supporting Information).

To summarise, ring closure in **3B** is kinetically demanding and connected with a substantial barrier of 29.2 kcal mol^{-1} ($\Delta G^{\neq}$) for the most accessible 6-*endo* pathway. DFT predicts that this pathway should be traversed almost exclusively, as the rival exocyclic pathway is kinetically impeded ($\Delta\Delta G^{\neq}$ gap of 7.4 kcal mol^{-1}). Thermodynamic grounds also favour the generation of the six-membered azacycle, which occurs in an irreversible fashion.

Protonolysis of azacyclic intermediates: Protonation of the azacyclic unit in **4B** and **5B**⇔**5B′** is encountered next in the course of the reaction. Various conceivable pathways have been critically explored (Scheme 4). The most accessible pathways, which are likely to be traversed in the catalytic process, are discussed in this section, whereas the full account of structural (Figures S2–S8) and energetic aspects (Table S2) of all the examined pathways is included in the Supporting Information.

*Intermediate **4B***: Considering firstly the protonolytic cleavage of the Zr–C^6 bond in **4B** by the substrate, the initial uptake of a substrate molecule leads to adduct **4B**-S, which has the amine rather loosely attached to Zr (Figure S2 in the Supporting Information). Amine association is facile,[20] but again, disfavoured in competition with the more strongly bound amido and azacycle ligands; hence **4B**-S is uphill in enthalpy and free energy relative to {**4B**+**1**} (Table 2). Proton transfer onto the C^6 centre of the azacycle's tether evolves through a TS structure constituting the simultaneous N–H bond cleavage and C–H bond formation. This process requires a free energy of activation of 32.3 kcal mol^{-1} (Table 2) and has an associated negative activation entropy of −20.0 cal mol^{-1} K^{-1} with respect to the entrance channel {**4B**+**1**}. Continuing further on this pathway leads to the liberation of cycloamine **P10**, thereby regenerating **3B**. This may well involve the transient cycloamine-bis(amido)-Zr species **6B**, which has the pyrrolidine weakly bond by its N-donor centre (Figure S2 in the Supporting Information). In-

Table 2. Enthalpies and free energies of activation and reaction for protonolysis of the azacycle-amido-Zr intermediates **4B** and **5B′** to afford cycloamine-bis(amido)-Zr compounds **6B**, **8B**, **9B** or cycloamine-imido-Zr compounds **7B**, **10B**, **11B** through various pathways for proton transfer.[a-c]

Proton transfer pathway[d]	**4B**/**5B′**-S[e]	TS	Product[e]
H transfer onto C^6 of **4B**			2-vinyl-pyrrolidine
4B+**1**→**6B**	9.4/15.4 (**4B**-S)	26.4/*32.3*	0.9/*6.5* (**6B**)
4B→**7B**		30.0/*29.6*	-1.4/*-2.8* (**7B**)
H transfer onto C^7 of **5B′**			6-methyl-tetrahydropyridine
5B′+**1**→**8B**	21.6/*27.5* (**5B′**-S)[g]	27.4/*34.3*[g]	–/– (**8B**)[h]
5B′→**10B**		27.8/*28.1*[g]	11.9/10.4 (**10B**)[g]
H transfer onto C^5 of **5B′**			2-methylene-piperidine
5B′+**1**→**9B**	10.6/*16.5* (**5B′**-S)[f]	22.1/*29.2*[f]	9.6/*15.1* (**9B**)[f]
5B′→**11B**		23.6/*23.7*[f]	10.6/*9.7* (**11B**)[f]
		Aminoallene substrate-assisted process[i]	
Proton transfer pathway[d]		TS	
H transfer onto C^6 of **4B**			
4B+**1**→**6B**		38.9/*50.3*	
4B→**7B**		32.0/*36.9*	
H transfer onto C^7 of **5B′**			
5B′+**1**→**8B**		36.0/*47.4*[g]	
5B′→**10B**		28.7/*34.5*[g]	
H transfer onto C^5 of **5B′**			
5B′+**1**→**9B**		28.2/*41.1*[f]	
5B′→**11B**		23.5/*28.7*[f]	

[a] See Scheme 4. [b] The activation barriers and reaction energies are given relative to the most stable form of the respective precursor species. [c] Enthalpies and free energies of activation ($\Delta H^{\neq}/\Delta G^{\neq}$) and reaction ($\Delta H/\Delta G$) are given in kilocalories per mole; the numbers in italic type are the Gibbs free energies. [d] The most accessible pathways are referred to. See also Table S2. [e] See the text (or Figure S2, S5) for description of the various isomers of amine adducts **4B**-S, **5B′**-S, and of the cycloamine-bis(amido)-Zr (**6B**, **8B**, **9B**) or cycloamine-imido-Zr (**7B**, **10B**, **11B**) product species. [f] The azacycle moiety is attached to Zr by its C^7 centre. [g] The azacycle moiety is attached to Zr by its C^5 centre. [h] All attempts to locate this species were unsuccessful. [i] The proton transfer has been studied in the presence of an additional methylamine ($MeNH_2$, S′) model substrate acting as a mediating "proton shuttle". Total barriers and reaction energies are relative to {**4B**+**1**+$MeNH_2$} and {**5B′**+**1**+$MeNH_2$}, respectively.

termediate **6B** decays afterwards almost instantaneously[20] into **3B**+**P10** ($\Delta G = -28.5$ kcal mol^{-1}), thus driving the overall **4B**+**1**→**3B**+**P10** protonolysis step strongly downhill.

Another proton transfer path without explicit amine participation is examined next and its key stationary points are shown in Figure 2. It can commence from the two isomers of **4B** generated through frontal and lateral cyclisation trajectories (see above). The most accessible pathway engages the former isomer (Table S2, Figure S3 in the Supporting Information), whereas cyclisation proceeds preferably through the lateral trajectory (see above). Accordingly, the two isomers of **4B** must interconvert prior to proton transfer, which is effectively realised through a kinetically less demanding rotation about the Zr–C^6 bond (Scheme 6).[27]

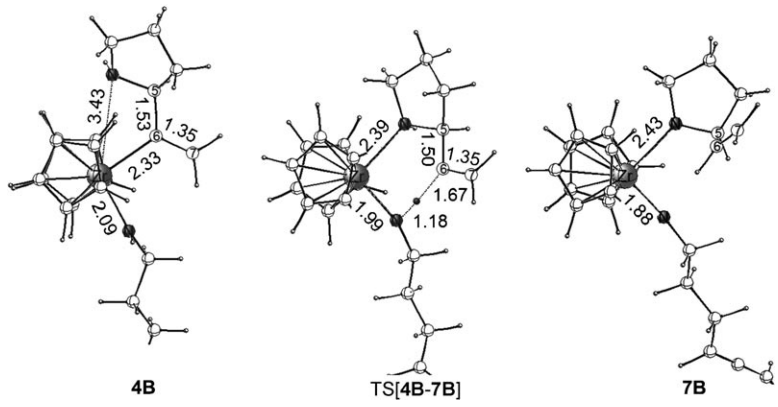

Figure 2. Selected structural parameters [Å] of the optimised structures of key stationary points for proton transfer in azacycle-amido-Zr intermediate **4B** to afford cycloamine-imido-Zr compound **7B**. The cut-off for drawing Zr–C bonds was arbitrarily set to 2.8 Å. Note that the amido/imidoallene unit is displayed in a truncated fashion for several of the species.

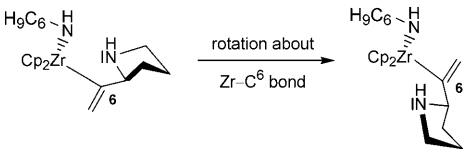

Scheme 6.

Following the minimum energy pathway to commence from **4B**, the C^6 carbon to be protonated becomes displaced from the immediate proximity of the metal upon traversing through the transition state. TS[**4B**-**7B**] features the transfer of an amido α-proton onto the vinylic tether that is accompanied by a partial amido→imido conversion and is stabilised by a closely attached azacycle by its N-donor centre (Figure 2). Decay of the transition state first leads to the cycloamine-imido-Zr compound **7B**, from which incoming **1** liberates pyrrolidine **P10** in a kinetically facile,[20] exergonic step ($\Delta G = -19.2$ kcal mol^{-1}). The initially regenerated **3A**-S is then converted into **3B** through an α-abstraction pathway (Scheme 3).

The activation enthalpy for **4B**→**7B** is somewhat larger when compared with **4B**+**1**→**6B** (Table 2). However, in contrast to the latter bimolecular step, the **4B**→**7B** pathway is not handicapped by the entropy costs for substrate participation. Hence, the amido α-proton abstraction (**4B**→**7B**, $\Delta G^{\ddagger} = 29.6$ kcal mol^{-1}) is the dominant path for protonolysis of **4B** to generate allylcycloamine **P10**.

A possible role of substrate has been gauged by employing methylamine as model substrate (S′). Given the already discussed electronic structure of the studied zirconocene compounds, it is rather unlikely that additional amine molecules can stabilise the metal centre by its association. In a more probable scenario, the amine may act instead as a mediating agent.[28] The associated TS structures feature the simultaneous protonation/deprotonation of an external molecule S′ bearing a formally quaternary nitrogen centre and reveal a concerted, but asynchronous proton transfer (Figure S6 in the Supporting Information). Considering the **4B**+**1**→**6B** and **4B**→**7B** pathways, the located transition states TS[**4B**-S-**6B**-S′] and TS[**4B**-**7B**-S′] are higher in enthalpy than {TS[**4B**-S-**6B**]+S′} and {TS[**4B**-**7B**]+S′}, respectively, and even more so in free energy. It may thus be concluded that excess amine acting as a "proton shuttle" is unlikely to accelerate the protonolysis of **4B**.

*Intermediates **5B**⇄**5B′***: The **5B**⇄**5B′** forms of the 6-*endo* azacyclic intermediate can be equally envisaged as precursor for the protonolysis step. Alternative pathways, with or without amine involvement, have been scrutinised and indicate that the most accessible pathways commence from the more stable **5B′** with a monohaptic allylic ligation of the azacycle. There is a preference for a η^1-C^7-azacycle ligation over the η^1-C^5-azacycle-Zr form ($\Delta G = 10.4$ kcal mol^{-1}), both of which are readily interconvertible.[26] The same order of stability is preserved in the substrate adduct **5B′**-S, which, comparable to **4B**-S, are transient species.

Several trajectories are conceivable for protonation of the azacycle, of which the following have been examined (Scheme 7): I) Protonolysis at the allylic η^1-azacycle-Zr bond and II) protonation at the remote allylic carbon that is opposite to the allylic η^1-azacycle-Zr linkage. Protonation of the azacycle, whereas it is bound by its N-donor centre, describes a third alternative.[29] The most accessible pathway evolves through a TS structure featuring proton transfer onto the unbound allylic centre and the azacycle is linked to Zr by its opposite allylic carbon (Table S2, Figures S4 and S5 in the Supporting Information). Hence, protonation at C^7 and C^5 carbons of **5B′** proceeds through TS structures

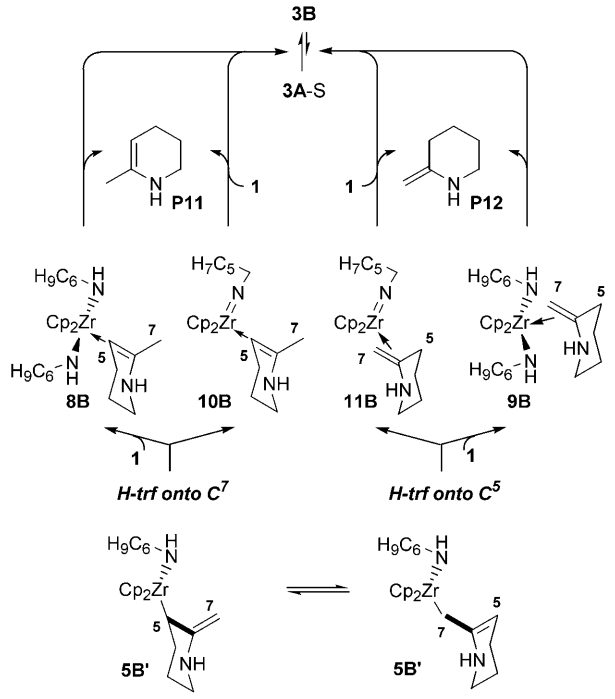

Scheme 7.

having the azacycle η^1-coordinated at C^5 and C^7 centres, respectively, thereby taking advantage of the stabilising influence of the bound azacycle. This preference for the various trajectories holds true irrespective of whether amine (**5B′**+**1**→**8B**/**9B**) or the amido group (**5B′**→**10B**/**11B**) serves as the proton source (Table S2 in the Supporting Information).

Similar to the findings for **4B**, α-proton abstraction from the amido group is the kinetically advantageous scenario against azacycle aminolysis. As revealed from Figure 3, the located TS structures for regioisomeric **5B′**→**10B** and **5B′**→**11B** pathways bear structural similarity to its counterpart discussed in the previous section for **4B** (Figure 2), featuring proton transfer onto the unbound allylic carbon together with a partially accomplished amido→imido transformation. The **5B′**→**11B** proton transfer onto the C^5 carbon appears as the most accessible of the various examined pathways with a computed free energy of activation of 23.7 kcal mol^{-1}. On the other hand, protonation at the C^7 centre to preferably proceed through **5B′**→**10B** is kinetically less feasible ($\Delta G^{\ddagger}$ = 28.1 kcal mol^{-1}, Table 2). Hence, DFT predicts that **5B′**→**11B** is predominantly traversed along the endocyclic branch, initially giving rise to **P12** in an overall exergonic step (ΔG = −13.4 kcal mol^{-1} for **5B′**→**11B** to be followed by **11B**+**1**→**3B**+**P12**). Piperidine **P12** is subsequently converted into the more stable cycloimine **P11′** by a 1,3-hydrogen shift (ΔG = −5.7 kcal mol^{-1}).[30]

With regards to the possible supportive effect of additive amine a scenario similar to that discussed above for **4B** has been assessed, in which model substrate S′ is functioning as a proton shuttle. The examination of the various pathways and trajectories revealed that the associated TS structures are not stabilised by an external S′ moiety at the free energy surface in either case (Table 2 and S2). Hence, added amine substrate does not appear to accelerate any of these pathways, which conforms to the findings for **4B**, and is therefore unlikely to assist the protonolysis of either **4B** or **5B**⇄**5B′**.

Free-energy profile: The condensed Gibbs free-energy profile, considering only viable pathways for relevant steps of the tentative catalytic cycle (Scheme 4) is displayed in Scheme 8. The following conclusions can be drawn: I) The $[Cp_2Zr(NHR)_2]$ complex **3B** bearing two η^1-amido groups is the catalytically active species that undergoes intramolecular insertion of an allenic C=C linkage into the Zr–NHR σ-bond. This complex represents the resting state of the cycle. II) Ring closure evolves through a chairlike TS structure for both regioisomeric pathways, which is not stabilised by close interactions between the unsaturated azacycle's tether functionality and Zr. Cyclisation in **3B** is kinetically demanding

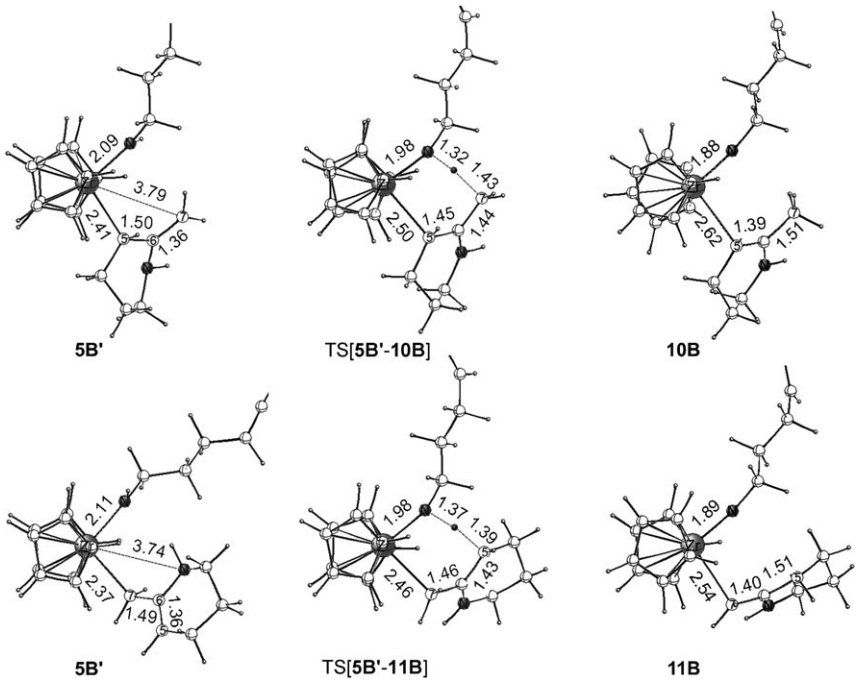

Figure 3. Selected structural parameters [Å] of the optimised structures of key stationary points for proton transfer in azacycle-amido-Zr intermediate **5B′** to afford cycloamine-imido-Zr compounds **10B**, **11B**. See Table S2 for the energetics. The cut-off for drawing Zr–C bonds was arbitrarily set to 2.8 Å. Note that the amido/imidoallene unit is displayed in a truncated fashion for several of the species.

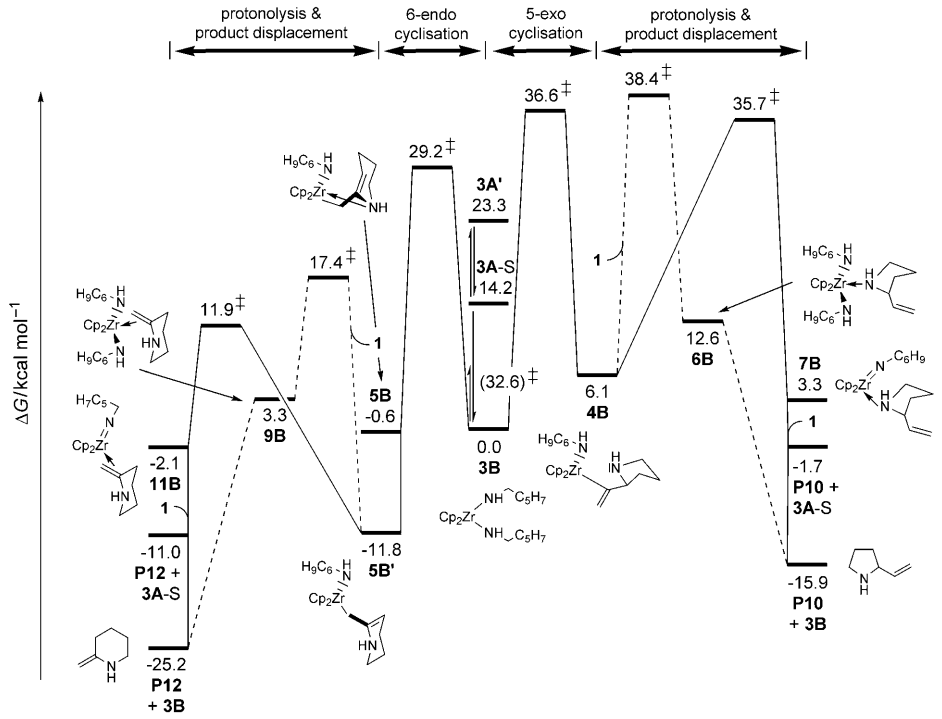

Scheme 8. Condensed Gibbs free-energy profile of the intramolecular hydroamination/cyclisation of **1** mediated by **2** to proceed through the $[Cp_2Zr(NHR)_2]$ complex **3B**. Note that **3B**⇔**3A**-S has a free energy of activation of 32.6 kcal mol^{-1} (Scheme 3). The most accessible pathways for individual steps are drawn by solid lines, whereas some alternative, but less favourable pathways are represented by dashed lines.

and excess substrate does not appear to assist this step. A free energy barrier of 29.2 kcal mol^{-1} is computed for the preferred endocyclic pathway that furnishes **5B′** in an overall exergonic process. III) α-Proton abstraction from the amido group is revealed as the dominant path for protonolysis of azacyclic intermediates **4B** and **5B′**. It proceeds through a TS structure featuring the concomitant amido N–H bond cleavage and C–H bond formation. External amine molecules acting as a mediating agent are not likely to accelerate the proton transfer step. Pyrrolidine **P10** is generated preferably by protonation at the vinylic C^6 centre of **4B** following the **4B**→**7B**(+**1**)→**3A**-S+**P10**→**3B**(+**P10**) pathway. Proton transfer onto the allylic C^5 carbon is most accessible for **5B′** initially giving rise to **P12** along **5B′**→**11B** (+**1**)→**3A**-S+**P12**→**3B**(+**P12**). Piperidine **P12** is readily converted afterwards into cycloimine **P11′**. IV) The reaction branch that commences with 6-*endo* cyclisation sees the highest barrier for ring closure ($\Delta G^{\ddagger}$ = 29.2 kcal mol^{-1}), whereas protonolysis is indicated to be more facile ($\Delta G^{\ddagger}$ = 23.7 kcal mol^{-1}). On the other hand, the computed total barrier (i.e. relative to **3B**) for cyclisation and protonation are of comparable magnitude along the branch that leads to **P10**. This, however, is of little relevance in further mechanistic discussions, since this branch is likely to remain almost closed throughout (see below). V) Accordingly, ring closure occurring in the thermodynamically prevalent **3B** is turnover limiting.

Elucidation of the regioselectivity: Within the mechanistic scenario analysed thus far, C=C insertion into the Zr–N σ-bond is the rate-limiting step that also controls the regioselectivity. Scheme 8 shows that the propensity of **3B** to undergo cyclisation following 5-*exo* and 6-*endo* pathways is distinctly different. The latter is favourable on both thermodynamic and kinetic grounds. Considering the computed kinetic gap of 7.4 kcal mol^{-1} ($\Delta\Delta G^{\ddagger}$), the exocyclic pathway appears to be kinetically prevented, thereby remaining inaccessible throughout the process, which therefore should proceed through the 6-*endo* pathway almost exclusively.[31] Accordingly, DFT predicts cycloimine **P12** as the sole product generated along the reaction channel that employs **3B** as the catalytically active species.

Reaction channel proceeding through the [Cp_2Zr=NR] intermediate: The reaction cycle involving the $[Cp_2Zr{=}NR]$ intermediate **3A′** as catalytically active species is shown in Scheme 9. It comprises accessible pathways for all relevant steps that have been recently identified by computational examination.[17] Commencing from **3A′**, an allenic C=C linkage adds across the Zr=NR bond through a [2+2] cycloaddition reaction. Ring closure can proceed through regioisomeric 5-*exo* and 6-*endo* paths, thereby affording azazirconacyclobutane intermediates **4A** and **5A** carrying five- and six-membered rings, respectively. Protonolytic cleavage of the metallacycle unit in **4A** and **5A** by **1** generates azacycle-amido-Zr compounds **6A**–**9A** following various pathways. Subsequent proton transfer from the amido-Zr unit onto the azacycle leads to cycloamine-imido-Zr complexes **10A**–**12A**, from which cycloamines **P10**–**P12** are liberated to regenerate **3A**-S⇔**3A′**+**1** and complete the cycle. Formation of allylcycloamine **P10** occurs preferably through protonolytic cleavage of the Zr–C^6 bond in **4A**, followed by α-hydrogen elimination.[17] The dominant route for the six-membered cycloimine involves protonolysis of the cyclobutane unit in **5A** at the Zr–N bond and subsequent proton transfer onto the azacycle's C^5 centre.[17] This leads initially to **P12**, which is likely to be readily transformed into the thermodynamically more stable **P11′**.

Free-energy profile: This reaction channel has been previously scrutinised in a detailed manner,[17] and its free energy

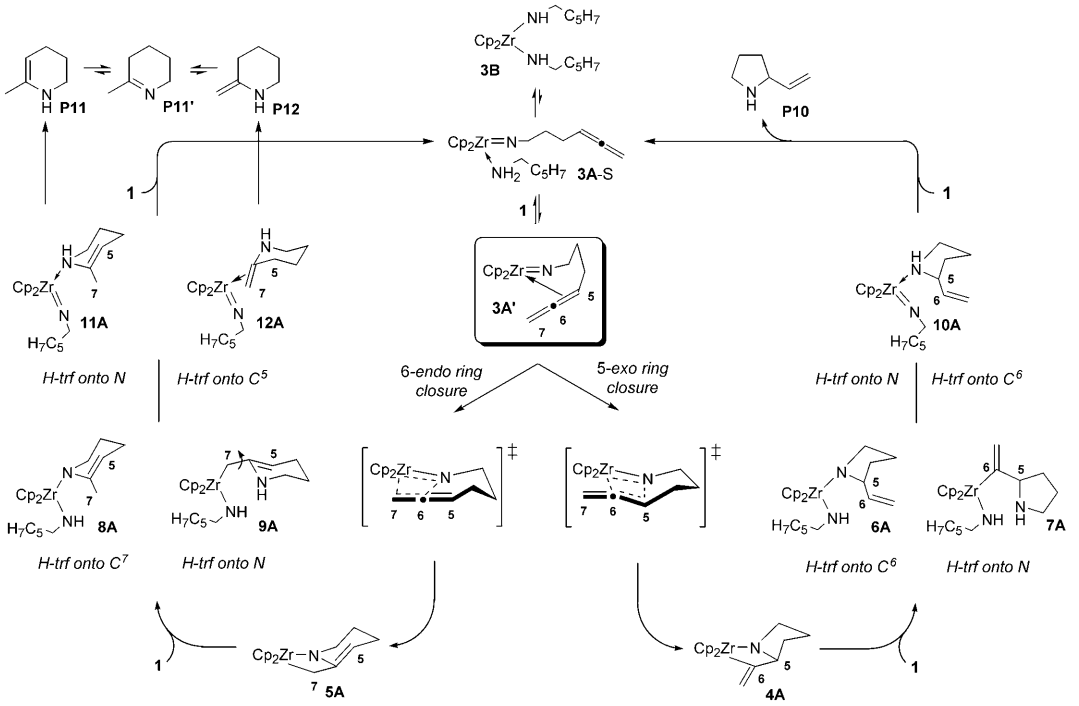

Scheme 9. Reaction channel proceeding through the imido-zirconocene intermediate **3A′** in aminoallene IHC to afford functionalised five- and six-membered azacycles, based on experimental[2b,6,8,9a] and computational[10,17] mechanistic studies.[32]

profile is shown in Scheme 10.[18] Important mechanistic conclusions derived from this Scheme are briefly summarised here. I) Transient species **3A′** is the catalytically active species that directly undergoes [2+2] cycloaddition. II) Ring closure has small intrinsic barriers of comparable magnitude associated to 5-*exo*- and 6-*endo* pathways, thereby indicating it as a highly facile process. III) The stepwise protonation of azazirconacyclobutane intermediates **4A** and **5A** is substantially slower when compared with cycloaddition. The first protonolytic cleavage of the azazirconacyclobutane unit is less demanding kinetically than the second protonation step. Excess substrate appears to accelerate the favourable pathways of the second step. IV) The most accessible route for generation of the five-membered allylamine involves **4A**+**1**→**6A** protonolytic metallacycle cleavage at the Zr–C^6 bond and subsequent **6A**→**10A** (+**1**)→**3A**-S+**P10** α-proton elimination. On the other hand, protonolysis of **5A** at the Zr–N linkage to be followed by proton transfer onto azacycle's C^5 centre in **9A** is the dominant path towards the six-membered imine (**5A**+**1**→**9A**→**12A**(+**1**)→**3A**-S+**P12**⇄**P11′**).

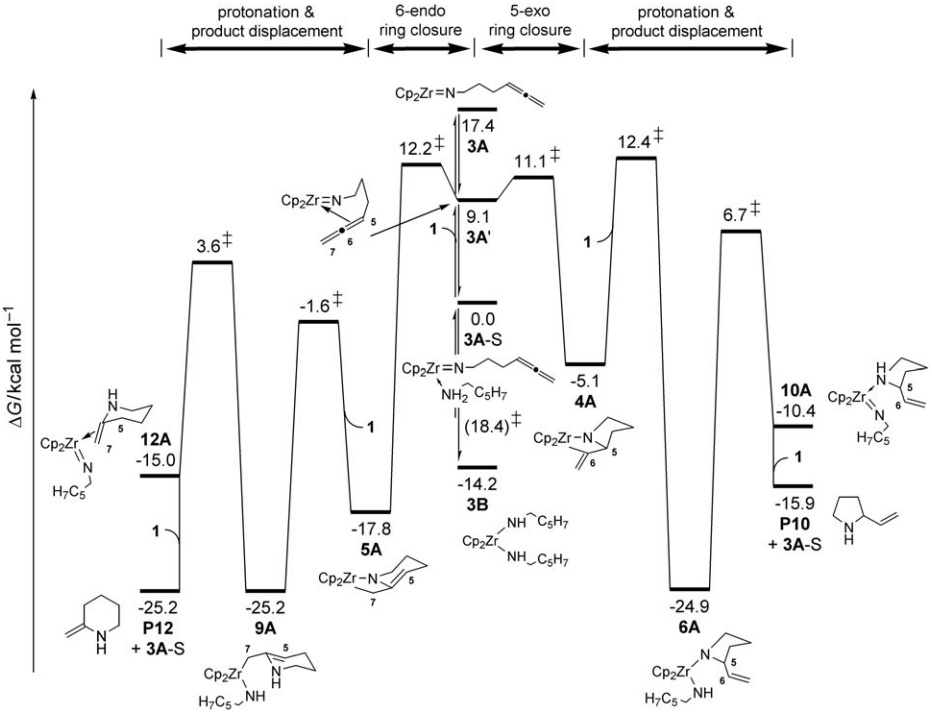

Scheme 10. Condensed Gibbs free-energy profile of the intramolecular hydroamination/cyclisation of **1** mediated by **2** to proceed through the [Cp_2Zr=NR] intermediate **3A′**. Note that **3A**-S⇔**3B** has a free-energy barrier of 18.4 kcal mol^{-1} (Scheme 3). Only the most accessible pathways for individual steps are included, whereas alternative, but less favourable pathways are omitted for the sake of clarity. See ref.[17] for full details.

V) Effective catalysis entails the conversion of the dormant complex **3B** first into the highly reactive, transient species **3A′**. The **3B**⇄**3A**-S⇄**3A′**+**1** transformation is turnover limiting ($\Delta G^{\neq}=32.6$ kcal mol^{-1}, Scheme 3) and **3A′**, which immediately undergoes cycloaddition, becomes regenerated after each successful loop through the cycle. This scenario is similar to the mechanism established for the Zr-catalysed intermolecular hydroamination of alkynes and allenes with primary amines.[8] The kinetically most demanding step of the productive cycle (i.e., **9A**→**12A** along the predominantly traversed branch) has a somewhat lower barrier ($\Delta G^{\neq}=$ 28.8 kcal mol^{-1}, Scheme 10).

Elucidation of the regioselectivity: The two branches towards generation of five-ring and six-ring cycloamines are linked together by the [2+2] cycloaddition, but proceed independently afterwards. Consequently, this step regulates the regioselective outcome. Ring closure is highly facile and has a small intrinsic barrier of 2.0 and 3.1 kcal mol^{-1} for 5-*exo* and 6-*endo* pathways, respectively. This disparity would indicate that **P10** is the predominant product together with a minor proportion of **P11′**.[33] It relies, however, on the circumstance that both pathways are driven by a comparable thermodynamic force, which turns out not to be the case. Ring closure along **3A′**→**5A** is strongly downhill and hence irreversible (Scheme 10). On the other hand, **4A** is formed in a less exergonic process and its consumption (**4A**+**1**→**6A**) has a comparable, but somewhat higher barrier than **4A**→**3A′** cyclorevision. In contrast to irreversible 6-*endo* ring closure, the 5-*exo* pathway is reversible. The kinetic model shown in Scheme 11 is employed for the assessment of the regioselectivity. It predicts that **P11′** is prevalent and is together with **P10** among the reaction products in a 61:39 ratio.[34]

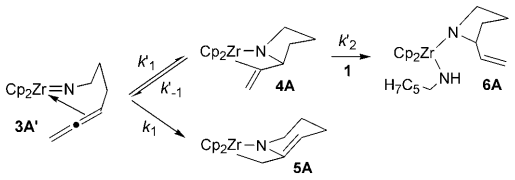

Scheme 11. Kinetic Scheme for the prediction of the regioselectivity for the reaction channel that proceeds through the [Cp_2Zr=NR] intermediate **3A′**.

exception of irreversible cycloaddition and product expulsion (see Scheme 10) and applying steady-state concentrations[35] for **3A**-S, **3A′**, **5A**, **9A** and **12A** yields a rate law ($\nu \sim [\mathbf{3B}][\mathbf{1}]^{-1}$),[34] which predicts first-order and inverse first-order dependence in [**3B**] and substrate concentration. This channel can thus display a rate increase at low substrate concentration and a rate decrease at high substrate concentration, owing to acceleration and inhibition of [Cp_2Zr=NR] formation via **3B**⇄**3A**-S⇄**3A′**+**1**, respectively.

The rival route that involves the [$Cp_2Zr(NHR)_2$] complex **3B** as the catalytically active species features turnover-limiting C=C insertion into the Zr–C σ-bond of **3B**, which represents the catalyst resting state. On the other hand, protonolysis is the more facile step in this case. This scenario is described by a simple rate law ($\nu \sim [\mathbf{3B}]$),[34] and accordingly substrate concentration is unlikely to influence the rate.

The likelihood of traversing the competing routes under a true catalytic regime is dictated by its associated turnover frequency. The TOF of a steady state catalytic system is determined by the free-energy span δG_{max} (with $r \sim \exp(-\delta G_{max}/RT)$) between the highest energy transition

Comparison of alternative reaction channels: Below is a summary of the prominent features of the rival IHC routes that are revealed from the mechanistic analysis thus far (Scheme 12).

The channel proceeding through the [Cp_2Zr=NR] intermediate entails first the conversion of dormant **3B** into highly reactive, transient **3A′** to traverse the cycle. The **3B**⇄**3A**-S⇄**3A′**+**1** transformation is turnover limiting and **3B** must be considered as the catalyst resting state. Protonolysis is the kinetically most demanding step ($k_{prot} < k'_{prot}$) in the productive cycle, whereas [2+2] cycloaddition (k_{clos}) is highly facile. Kinetic analysis, assuming all steps to be reversible, with the

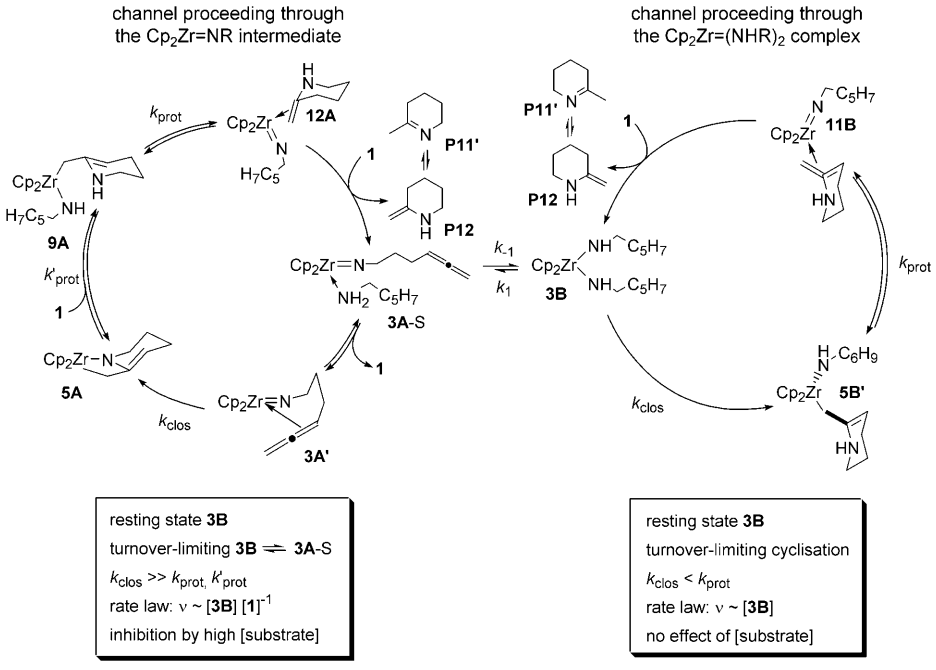

Scheme 12. Rival IHC routes revealed by mechanistic analysis.

state and the most stable intermediate preceding it.[36] An efficient process should display the smallest possible value for δG_{max}. We apply this concept to the free-energy profiles shown in Scheme 8 and 10 following a recently reported procedure.[37] The [Cp_2Zr=NR] cycloaddition route has a free-energy span of 32.6 kcal mol^{-1} (between TS[**3B**-**3A**-S] and **3B**), whereas δG_{max} amounts to 29.2 kcal mol^{-1} (between TS[**3B**-**5B**] and **3B**) for the [$Cp_2Zr(NHR)_2$] σ-bond insertion route. The small disparity in δG_{max} renders any firm conclusion about which of the routes is operative difficult to make. It does, however, indicate that the two routes are energetically very similar, and therefore equally viable for the type of hydroamination catalysis studied here, such that neither mechanism can be discarded a priori from a mechanistic analysis.

The IHC of **1** by **2** has been reported to furnish cycloimine **P11′** predominantly together with allylamine **P10** as a minor product.[15b] This is consistent with the characteristics of the [Cp_2Zr=NR] cycloaddition route (see above). The computationally predicted 61:39 composition of **P11′**:**P10** products compares favourably with the observed 84:16 ratio (Scheme 1). On the other hand, **P11′** should be generated as the sole product through the σ-bond insertion route.[31] This leads one to conclude that the Zr=N [2+2] cycloaddition route involving the [Cp_2Zr=NR] intermediate **3A′** is most probably traversed in the IHC of aminoallene **1** by [Cp_2ZrMe_2] precatalyst **2**. The Zr–N σ-bond insertion pathway appears not to be employed in the present case, but is clearly indicated as a viable mechanism for IHC of various unsaturated carbon–carbon linkages mediated by neutral organozirconium compounds and can perhaps be favourable in other cases. The delicate balance discovered between the alternative routes can be significantly influenced by the nature of the unsaturated carbon–carbon functionality, the size and accessibility of the Group 4 metal, the electronic and steric properties of spectator ligands and, of course, the substitution pattern at the nitrogen centre. These aspects will be the subject of further exploration.

Concluding Remarks

Presented herein is a computational study of alternative reaction channels for intramolecular hydroamination/cyclisation (IHC) of a prototypical primary aminoallene mediated by a charge neutral zirconocene precatalyst. Firstly, the route that uses [$Cp_2Zr(NHR)_2$] as the reactive species, involves the insertion of an allenic C=C linkage into the Zr–NHR σ-bond and subsequent protonolysis, has been explored and its key features have been defined. This route has been compared to the [2+2] cycloaddition path proceeding via an [Cp_2Zr=NR] intermediate. The salient features of the rival mechanisms are disclosed and critically compared with experiment. This detailed insight provides a rationale for the difference in product regioselectivity of the two mechanisms. The present study is indicative of an operating [2+2] cycloaddition mechanism, whereas the Zr–N σ-bond insertion mechanism appears not to be employed for the present case. The mechanistic analysis does, however, clearly indicate the Zr–N σ-bond insertion route is viable for IHC of amine-tethered unsaturated carbon-carbon linkages by charge neutral organozirconium compounds, and this corroborates recent experimental discoveries.[13,14] Overall, the findings disclosed herein provide additional insight into fundamental aspects of hydroamination mediated by early metals and may facilitate further advances in this area.

Computational Methods

All DFT calculations were performed by means of the program package TURBOMOLE[38] using the TPSS density functional[39] within the RI-*J* approximation[40] in conjunction with flexible basis sets of triple-ζ quality. For Zr we used the Stuttgart–Dresden quasirelativistic effective core potential (SDD) with the associate (8s7p6d)/[6s5p3d] valence basis set contracted according to a (311111/22111/411) scheme.[41] All other elements were represented by Ahlrich's valence triple-ζ TZVP basis set[42] with polarization functions on all atoms. The good to excellent performance of the TPSS functional for a wide range of applications has been demonstrated previously.[43] The growing string method[44] was employed for exploring of reaction paths, in which two string fragments (commencing from reactant and product side, respectively) are grown until the two fragments join. As this was performed in mass-weighted coordinates, an approximate to the minimum energy path (MEP) was obtained. This identified the reactant and product states to be linked to the associated transition state. The approximate saddle point connected with the MEP was subjected to an exact localisation of the TS structure. All stationary points were located by utilizing analytical/numerical gradients/Hessians according to standard algorithms and were identified exactly by the curvature of the potential-energy surface at these points corresponding to the eigenvalues of the Hessian. The gas-phase reaction and activation enthalpies and free energies (ΔH, $\Delta H^{\neq}$ and ΔG, $\Delta G^{\neq}$ at 298 K and 1 atm) were evaluated according to standard textbook procedures[45] by using computed harmonic frequencies. Enthalpies were reported as ΔE+zero-point-energy corrections at 0 K+thermal-motion corrections at 298 K and Gibbs free-energies were obtained as $\Delta G = \Delta H - T\Delta S$ at 298 K. The influence of the solvent was taken into explicit consideration by making use of a continuum model. The experimentally used benzene solvent[15b] was described as a homogeneous, isotropic dielectric medium (characterised by its relative static dielectric permittivity $\varepsilon = 2.247$ at 298 K)[46] within the conductor-like screening model (COSMO) due to Klamt and Schüürmann[47] as implemented in TURBOMOLE.[48] Nonelectrostatic contributions to solvation were not included. The solvation effects were included self-consistently, and all the key species were fully located with inclusion of solvation. The solvation enthalpy was approximated by the difference between the electronic energy computed by using the COSMO solvation model and the gas-phase energy. The entropy contributions for condensed-phase conditions were estimated on the basis of the computed gas-phase entropies by employing the procedure of Wertz.[49] Further details of the computational methodology employed are given in the Supporting Information. The mechanistic conclusions drawn in this study were based on the computed Gibbs free-energy profile of the overall reaction for experimental condensed phase conditions. All the drawings were prepared by employing the StrukEd program.[50]

[1] For reviews of catalytic hydroamination, see: a) L. S. Hegedus, *Angew. Chem.* **1988**, *100*, 1147; *Angew. Chem. Int. Ed.* **1988**, *27*, 1113; b) D. M. Roundhill, *Catal. Today* **1997**, *37*, 155; c) T. E. Müller, M. Beller, *Chem. Rev.* **1988**, *98*, 675; d) M. Nobis, B. Driessen-Hölscher, *Angew. Chem.* **2001**, *113*, 4105; *Angew. Chem. Int. Ed.* **2001**, *40*, 3983; e) R. Taube in *Applied Homogeneous Catalysis with Organometallic Complexes* (Eds.: B. Cornils, W. A. Herrmann),

Wiley-VCH, Weinheim, **2002**; pp. 513–524; f) J. Seayad, A. Tillack, C. G. Hartung, M. Beller, *Adv. Synth. Catal.* **2002**, *344*, 795; g) F. Pohlki, S. Doye, *Chem. Soc. Rev.* **2003**, *32*, 104; h) P. W. Roesky, T. E. Müller, *Angew. Chem.* **2003**, *115*, 2812; *Angew. Chem. Int. Ed.* **2003**, *42*, 2708; i) J. F. Hartwig, *Pure Appl. Chem.* **2004**, *76*, 507; j) K. C. Hultzsch, *Adv. Synth. Catal.* **2005**, *347*, 367; k) A. L. Odom, *Dalton Trans.* **2005**, 225; l) R. Severin, S. Doye, *Chem. Soc. Rev.* **2007**, *36*, 1407.

[2] For cyclohydroamination mediated by charge-neutral Group 4 metal complexes; see: a) P. L. McGrane, T. Livinghouse, *J. Org. Chem.* **1992**, *57*, 1323; b) P. L. McGrane, M. Jensen, T. Livinghouse, *J. Am. Chem. Soc.* **1992**, *114*, 5459; c) P. L. McGrane, T. Livinghouse, *J. Am. Chem. Soc.* **1993**, *115*, 11485; d) I. Bytschkov, S. Doye, *Tetrahedron Lett.* **2002**, *43*, 3715; e) C. Li, R. K. Thomson, B. Gillon, B. O. Patrick, L. L. Schafer, *Chem. Commun.* **2003**, 2462; f) J. A. Bexrud, J. D. Beard, D. C. Leitch, L. L. Schafer, *Org. Lett.* **2005**, *7*, 1959; g) H. Kim, P. H. Lee, T. Livinghouse, *Chem. Commun.* **2005**, 5205; h) A. Heutling, F. Pohlki, I. Bytschkov, S. Doye, *Angew. Chem.* **2005**, *117*, 3011; *Angew. Chem. Int. Ed.* **2005**, *44*, 2951; i) R. K. Thomson, J. A. Bexrud, L. L. Schafer, *Organometallics* **2006**, *25*, 4069; j) C. Müller, C. Loos, N. Schulenburg, S. Doye, *Eur. J. Org. Chem.* **2006**, 2499; k) D. A. Watson, M. Chiu, R. G. Bergman, *Organometallics* **2006**, *25*, 4731; l) M. C. Wood, D. C. Leitch, C. S. Yeung, J. A. Kozak, L. L. Schafer, *Angew. Chem.* **2007**, *119*, 358; *Angew. Chem. Int. Ed.* **2007**, *46*, 354; m) L. Ackermann, L. T. Kaspar, A. Althammer, *Org. Biomol. Chem.* **2007**, *5*, 1975.

[3] For cyclohydroamination mediated by cationic Group 4 metal complexes; see: a) D. V. Gribkov, K. C. Hultzsch, *Angew. Chem.* **2004**, *116*, 5659; *Angew. Chem. Int. Ed.* **2004**, *43*, 5542; b) P. A. Knight, I. Munslow, P. N. O'Shaughnessy, P. Scott, *Chem. Commun.* **2004**, 894.

[4] a) T. J. Marks, R. D. Ernst, in *Comprehensive Organometallic Chemistry* (Eds.: G. Wilkinson, F. G. A. Stone, E. W. Abel), Pergamon Press, Oxford, **1982**, Chap. 21; b) W. J. Evans, *Adv. Organomet. Chem.* **1985**, *24*, 131; c) C. J. Schaverien, *Adv. Organomet. Chem.* **1994**, *36*, 283; d) H. Schumann, J. A. Meese-Marktscheffel, L. Esser, *Chem. Rev.* **1995**, *95*, 865; e) F. T. Edelmann, in *Comprehensive Organometallic Chemistry* (Eds.: G. Wilkinson, F. G. A. Stone, E. W. Abel), Pergamon Press, Oxford, **1995**, Chap. 2; f) R. Anwander, W. A. Herrmann, *Top. Curr. Chem.* **1996**, *179*, 1; g) F. T. Edelmann, *Top. Curr. Chem.* **1996**, *179*, 247; h) *Topics in Organometallic Chemistry, Vol. 2* (Ed.: S. Kobayashi), Springer, Berlin, **1999**; i) M. N. Bochkarev, *Chem. Rev.* **2002**, *102*, 2089; j) S. Arndt, J. Okuda, *Chem. Rev.* **2002**, *102*, 1953; k) F. T. Edelmann, D. M. M. Freckmann, H. Schumann, *Chem. Rev.* **2002**, *102*, 1851; l) H. C. Aspinall, *Chem. Rev.* **2002**, *102*, 1807.

[5] For cyclohydroamination mediated by organolanthanides, see: a) M. R. Gagné, T. J. Marks, *J. Am. Chem. Soc.* **1989**, *111*, 4108; b) M. R. Gagné, T. J. Marks, *J. Am. Chem. Soc.* **1992**, *114*, 275; c) Y. Li, P.-F. Fu, T. J. Marks, *Organometallics* **1994**, *13*, 439; d) Y. Li, T. J. Marks, *J. Am. Chem. Soc.* **1996**, *118*, 9295; e) G. A. Molander, E. D. Dowdy, *J. Org. Chem.* **1998**, *63*, 8983; f) M. R. Bürgstein, H. Berberich, P. W. Roesky, *Organometallics* **1998**, *17*, 1452; g) A. T. Gilbert, B. L. Davis, T. J. Emge, R. D. Broene, *Organometallics* **1999**, *18*, 2125; h) G. A. Molander, E. D. Dowdy, *J. Org. Chem.* **1999**, *64*, 6515; i) Y. K. Kim, T. Livinghouse, J. E. Bercaw, *Tetrahedron Lett.* **2001**, *42*, 2944; j) G. A. Molander, E. D. Dowdy, S. K. Pack, *J. Org. Chem.* **2001**, *66*, 4344; k) M. R. Bürgstein, H. Berberich, P. W. Roesky, *Chem. Eur. J.* **2001**, *7*, 7078; l) S. Hong, T. J. Marks, *J. Am. Chem. Soc.* **2002**, *124*, 7886; m) S. Hong, S. Tian, M. V. Metz, T. J. Marks, *J. Am. Chem. Soc.* **2003**, *125*, 14768; n) A. Zulys, T. K. Panda, M. T. Gamer, P. W. Roesky, *Chem. Commun.* **2004**, 2584.

[6] Cyclohydroamination of aminoallenes by titanium tetrakisamido, zirconium bis(sulfonamido) and zirconocene compounds: a) L. Ackermann, R. G. Bergman, *Org. Lett.* **2002**, *4*, 1475; b) L. Ackermann, R. G. Bergman, R. N. Loy, *J. Am. Chem. Soc.* **2003**, *125*, 11956.

[7] Cyclohydroamination of aminoallenes by titanium amino-alcohol compounds: a) J. M. Hoover, J. R. Petersen, J. M. Pikul, A. R. Johnson, *Organometallics* **2004**, *23*, 4614; b) J. R. Petersen, J. M. Hoover, W. S. Kassel, A. L. Rheingold, A. R. Johnson, *Inorg. Chim. Acta* **2005**, *358*, 687.

[8] a) P. J. Walsh, A. M. Baranger, R. G. Bergman, *J. Am. Chem. Soc.* **1992**, *114*, 1708; b) A. M. Baranger, P. J. Walsh, R. G. Bergman, *J. Am. Chem. Soc.* **1993**, *115*, 2753; c) S. Y. Lee, R. G. Bergman, *Tetrahedron* **1995**, *51*, 4255; d) J. S. Johnson, R. G. Bergman, *J. Am. Chem. Soc.* **2001**, *123*, 2923.

[9] a) F. Pohlki, S. Doye, *Angew. Chem.* **2001**, *113*, 2361; *Angew. Chem. Int. Ed.* **2001**, *40*, 2305; b) Y. Li, Y. Shi, A. L. Odom, *J. Am. Chem. Soc.* **2004**, *126*, 1794; c) B. D. Ward, A. Maisse-Francois, P. Mountford, L. H. Gade, *Chem. Commun.* **2004**, 704.

[10] B. F. Straub, R. G. Bergman, *Angew. Chem.* **2001**, *113*, 4768; *Angew. Chem. Int. Ed.* **2001**, *40*, 4632.

[11] S. Hong, T. J. Marks, *Acc. Chem. Res.* **2004**, *37*, 673.

[12] S. Tobisch, *Dalton Trans.* **2006**, 4277.

[13] B. D. Stubbert, T. J. Marks, *J. Am. Chem. Soc.* **2007**, *129*, 6149.

[14] A recent study of aminoalkene IHC catalysed by neutral zirconium dipyrrolmethane compounds came to a similar conclusion: S. Majumder, A. L. Odom, *Organometallics* **2008**, *27*, 1174.

[15] Cyclohydroamination of aminoallenes by titanium tetrakisamido, zirconium bis(sulfonamido) and zirconocene compounds: a) L. Ackermann, R. G. Bergman, *Org. Lett.* **2002**, *4*, 1475; b) L. Ackermann, R. G. Bergman, R. N. Loy, *J. Am. Chem. Soc.* **2003**, *125*, 11956.

[16] Cyclohydroamination of aminoallenes by titanium amino-alcohol compounds: a) J. M. Hoover, J. R. Petersen, J. M. Pikul, A. R. Johnson, *Organometallics* **2004**, *23*, 4614; b) J. R. Petersen, J. M. Hoover, W. S. Kassel, A. L. Rheingold, A. R. Johnson, *Inorg. Chim. Acta* **2005**, *358*, 687.

[17] S. Tobisch, *Chem. Eur. J.* **2007**, *13*, 4884.

[18] Note that the energetics is slightly different from what has been communicated in ref. [17] in which the BP86 functional was employed.

[19] a) P. J. Walsh, F. J. Hollander, R. G. Bergman, *Organometallics* **1993**, *12*, 3705; b) A. P. Duncan, R. G. Bergman, *Chem. Rec.* **2002**, *2*, 431.

[20] Examination by a linear-transit approach gave no indication that this process is associated with a significant enthalpic barrier.

[21] A rate constant of $\approx 5\times10^{-5}\,s^{-1}$ (358.15 K) has been reported for thermolysis of the (4-*tert*-butylanilido)methyl-zirconocene complex to yield the bis(4-*tert*-butylanilido)-zirconocene complex in the presence of 4-*tert*-butylaniline (see ref. [18a]). This transforms into a barrier of 28.1 kcal mol^{-1} ($\Delta G^{\neq}$) for the kinetically most demanding step, which is, according to Scheme 3, **I1**→**3A′**+CH_4.

[22] It should be noted that steric bulk at the nitrogen centre is known to greatly affect the relative stability of species **3A**, **3A′**, **3A**-S, **3AD**, **3B** and also the kinetics of α-elimination (see, for instance, ref. [9a,10]).

[23] Scheme 4 displays plausible protonolysis pathways to furnish cycloamine-bis(amido)-Zr and cycloamine-imido-Zr intermediates for **4B**, whereas the former are omitted for **5B**⇄**5B′** for the sake of clarity.

[24] J. W. Lauher, R. Hoffmann, *J. Am. Chem. Soc.* **1976**, *98*, 1729.

[25] a) M. R. Gagné, L. Brard, V. P. Conticello, M. A. Giardello, C. L. Stern, T. J. Marks, *Organometallics* **1992**, *11*, 2003; b) G. A. Molander, J. A. C. Romero, *Chem. Rev.* **2002**, *102*, 2161.

[26] The interconversion of η^1-C^7-azacycle-Zr and η^1-C^5-azacycle-Zr isomers of **5B′** proceeds through an η^3-allylic intermediate, which has been examined by a linear-transit approach.

[27] The rotational process has been examined in a linear transit fashion by varying a dihedral angle about the Zr–C^6 bond, which led to an estimated barrier of 7.4 kcal mol^{-1}.

[28] a) H. M. Senn, P. E. Blöchl, A. Togni, *J. Am. Chem. Soc.* **2000**, *122*, 4098; b) S. Ilieva, B. Gabalov, D. G. Musaev, K. Morokuma, H. F. Schaefer, III, *J. Org. Chem.* **2003**, *68*, 1496.

[29] Despite several attempts a transition state could not be located for this trajectory, but indicated that it would be at high energy, and therefore unlikely to be involved along the minimum energy pathway. This again reflects the reduced abilities of the azacycle's N-donor centre to compete for coordination with other more strongly bond ligands.

[30] The 1,3-hydrogen shift is presumably a viable process. The kinetics of this process has not been investigated in the present study.
[31] Note that DFT is capable of predicting the relative kinetics of stereoisomeric pathways in high accuracy (that is with a disparity of less than 1 kcal mol^{-1}). See, for instance , a) S. Tobisch, T. Ziegler, *J. Am. Chem. Soc.* **2002**, *124*, 13290; b) S. Tobisch, *Chem. Eur. J.* **2003**, *9*, 1217; c) S. Tobisch, T. Ziegler, *J. Am. Chem. Soc.* **2004**, *126*, 9059. The computed free energy gap of 7.4 kcal mol^{-1} therefore allows one to conclude with some confidence that allylamine **P10** is not among the products for the σ-bond insertion reaction channel.
[32] Scheme 9 comprises accessible pathways for protonolysis of intermediates **4A** and **5A**. See ref. [17] for a detailed computational scrutiny of an almost complete set of alternative pathways for relevant steps in aminoallene IHC.
[33] The assessed $\Delta\Delta G^{\neq}$ gap of 1.1 kcal mol^{-1} corresponds to a **P10**:**P11′** ratio of 86:14 (298.15 K) on application of Maxwell–Boltzmann statistics.
[34] See the Supporting Information for more details.
[35] J. H. Espenson, *Chemical Kinetics and Reaction Mechanisms*, 2nd ed.; McGraw–Hill: New York, **1995**.
[36] a) J. A. Christiansen, *Adv. Catal.* **1953**, *5*, 311; b) C. Amatore, A. Jutand, *J. Organomet. Chem.* **1999**, *576*, 254.
[37] a) S. Kozuch, C. Amatore, A. Jutand, S. Shaik, *Organometallics* **2005**, *24*, 2319; b) S. Kozuch, S. Shaik, *J. Am. Chem. Soc.* **2006**, *128*, 3355.
[38] a) R. Ahlrichs, M. Bär, M. Häser, H. Horn, C. Kölmel, *Chem. Phys. Lett.* **1989**, *162*, 165; b) O. Treutler, R. Ahlrichs, *J. Chem. Phys.* **1995**, *102*, 346.
[39] a) P. A. M. Dirac, *Proc. Royal Soc. (London)* **1929**, *A123*, 714; b) J. C. Slater, *Phys. Rev.* **1951**, *81*, 385; c) J. P. Perdew, Y. Wang, *Phys. Rev.* **1992**, *B45*, 13244; d) J. Tao, J. P. Perdew, V. N. Staroverov, G. E. Scuseria, *Phys. Rev. Lett.* **2003**, *91*, 146401; e) J. P. Perdew, J. Tao, V. N. Staroverov, G. E. Scuseria, *J. Chem. Phys.* **2004**, *120*, 6898.
[40] a) O. Vahtras, J. Almlöf, M. W. Feyereisen, *Chem. Phys. Lett.* **1993**, *213*, 514; b) K. Eichkorn, O. Treutler, H. Öhm, M. Häser, R. Ahlrichs, *Chem. Phys. Lett.* **1995**, *242*, 652.
[41] D. Andrae, M. Häussermann, M. Dolg, H. Stoll and H. Preuss, *Theor. Chim. Acta* **1990**, *77*, 123.
[42] A. Schäfer, C. Huber, R. Ahlrichs, *J. Chem. Phys.* **1994**, *100*, 5829.
[43] a) V. N. Staroverov, G. E. Scuseria, J. Tao, J. P. Perdew, *J. Chem. Phys.* **2003**, *119*, 12129; b) Y. Zao, D. G. Truhlar, *J. Chem. Theory Comput.* **2005**, *1*, 415; c) F. Furche, J. P. Perdew, *J. Chem. Phys.* **2006**, *124*, 044103.
[44] a) B. Peters, A. Heyden, A. T. Bell, A. Chakraborty, *J. Chem. Phys.* **2004**, *120*, 7877; b) A. Heyden, *personal communication*.
[45] D. A. McQuarrie, Statistical Thermodynamics, Harper & Row, New York, **1973**.
[46] CRC Handbook of Chemistry and Physics, 84th ed. (Ed.: D. R. Lide), CRC Press, New York, **2003**–**2004**.
[47] a) A. Klamt, G. Schüürmann, *J. Chem. Soc. Perkin Trans. 2* **1993**, 799; b) A. Klamt in *Encyclopedia of Computational Chemistry, Vol. 1* (Ed.: P. von R. Schleyer), Wiley, Chichester, **1998**, pp. 604–615.
[48] A. Schäfer, A. Klamt, D. Sattel, J. C. W. Lohrenz and F. Eckert, *Phys. Chem. Chem. Phys.* **2000**, *2*, 2187.
[49] D. H. Wertz, *J. Am. Chem. Soc.* **1980**, *102*, 5316.
[50] For further details, see http://www.struked.de.

Received: April 20, 2008
Published online: August 7, 2008

